

Nitric Oxide Dioxygenation Reaction in DevS and the Initial Response to Nitric Oxide in *Mycobacterium tuberculosis*[†]

Erik T. Yukl,^{‡,||} Alexandra Ioanoviciu,[§] Santhosh Sivaramakrishnan,[§] Michiko M. Nakano,[‡] Paul R. Ortiz de Montellano,[§] and Pierre Moënne-Loccoz^{*,‡}

[‡]Division of Environmental and Biomolecular Systems, Oregon Health and Science University, 20000 Northwest Walker Road, Beaverton, Oregon 97006-8921, United States, and [§]Department of Pharmaceutical Chemistry, University of California, 600 16th Street, San Francisco, California 94158-2517, United States. ^{||}Current address: Department of Biochemistry, Molecular Biology and Biophysics, University of Minnesota, Minneapolis, MN 55455.

Received September 20, 2010; Revised Manuscript Received December 30, 2010

ABSTRACT: DevS and DosT from *Mycobacterium tuberculosis* (MTB) are paralogous heme-based sensor kinases that respond to hypoxia and to low concentrations of nitric oxide (NO). Both proteins work with the response regulator DevR as a two-component regulatory system to induce the dormancy regulon in MTB. While DevS and DosT are inactive when dioxygen is bound to the heme Fe(II) at their sensor domain, autokinase activity is observed in their heme Fe(II)–NO counterparts. To date, the conversion between active and inactive states and the reactivity of the heme–oxy complex toward NO have not been investigated. Here, we use stopped-flow UV–vis spectroscopy and rapid freeze quench resonance Raman spectroscopy to probe these reactions in DevS. Our data reveal that the heme–O₂ complex of DevS reacts efficiently with NO to produce nitrate and the oxidized Fe(III) heme through an NO dioxygenation reaction that parallels the catalytic reactions of bacterial flavohemoglobin and truncated hemoglobins. Autophosphorylation activity assays show that the Fe(III) heme state of DevS remains inactive but exhibits a high affinity for NO and forms an Fe(III)–NO complex that is readily reduced by ascorbate, a mild reducing agent. On the basis of these results, we conclude that upon exposure to low NO concentrations, the inactive oxy–heme complex of DevS is rapidly converted to the Fe(II)–NO complex in the reducing environment of living cells and triggers the initiation of dormancy.

Mycobacterium tuberculosis (MTB)¹ is able to survive hypoxia and exposure to NO, conditions thought to be prevalent within the host (1, 2), by undergoing a metabolic transformation to a state known as nonreplicating persistence. Entrance into this state is characterized by the induction of a regulon of around 50 genes, the so-called “dormancy regulon” (3–5), and is regulated by the response regulator DevR of the two-component regulatory system known as DevSRT (alternatively DosSRT) (6). DevR is activated when the paralogous sensor kinases DevS and DosT autophosphorylate and subsequently transfer the phosphate group to DevR (7). DevS and DosT use a bound heme cofactor to sense environmental conditions and are inactive when the heme Fe(II) binds O₂. They become active when the heme is in the Fe(II)–deoxy state, signaling hypoxia, or when it binds CO or NO (8–10). The Fe(III) state of DevS is also inactive (8, 10), while the activity of this state in DosT has not been reported.

Both sensors are required for wild-type levels of induction of the DevR regulon in response to both hypoxia (7) and NO exposure, as well as for survival (11) within the Wayne hypoxic model (2). Whether the effects of DevS and DosT are additive or whether they have specific roles in DevR activation is a question that has received significant attention. Two reports suggest that DevS acts as a redox sensor, whereas DosT is predominantly a sensor of hypoxia (8, 12). These conclusions, which are based on high rates of autoxidation of the DevS oxy complex relative to that of DosT, suggest that DevS is present in the Fe(III) form under aerobic conditions and requires the action of a reducing agent upon the transition into hypoxia. However, the reported rates of oxy-DevS autoxidation vary drastically. For example, one study reported that Fe(II) DevS converted directly to the Fe(III) form upon exposure to oxygen (8), whereas another determined a half-life of 4.1 h at 37 °C for oxy-DevS (9), or even as high as 210 h at 25 °C when transition metal ions were removed from the medium (13). The latter study also identified an endogenous electron donor protein that could efficiently reduce ferric DevS. In view of the large differences in measured autoxidation rates, and the demonstration that DevS and DosT are intrinsically stable to autoxidation, it is highly speculative to differentiate the *in vivo* functions of DevS and DosT by their relative susceptibility to autoxidation.

An attractive hypothesis for the respective roles of DevS and DosT is that these two sensor kinases provide separate temporal activation of DevR, because DevS is expressed from the dormancy

[†]This work was supported by Grants GM74785 (P.M.-L.) and AI074824 (P.R.O.d.M.) from the National Institutes of Health.

^{*}To whom correspondence should be addressed: Oregon Health and Science University, 20000 NW Walker Rd., Beaverton, OR 97006. Telephone: (503) 748-1673. Fax: (503) 748-1464. E-mail: plocco@ebf.org.edu.

¹Abbreviations: MTB, *Mycobacterium tuberculosis*; wt, wild-type; NOD, nitric oxide dioxygenation reaction; RR, resonance Raman; EPR, electron paramagnetic resonance; FTIR, Fourier transform infrared; RFQ, rapid freeze quench; HS/LS, high-spin/low-spin.

regulon controlled by DevR (5) while the expression level of DosT is unaffected by DevR or changes in O₂ concentration (4, 11, 14). The inference is that DosT acts in the early response of MTB to NO exposure or hypoxia, thus upregulating expression of DevS for further response amplification. Indeed, analysis of dormancy regulon expression in DevS and DosT deletion strains, in response to anaerobic conditions, shows DosT to be responsible for ~60% of induction relative to that of wt after 4 h but only 7% after 6 days (11). In contrast, the response of each deletion mutant to NO was equivalent, with ~20% of induction relative to that of wt after aerobic incubation with a NO donor for 1 h. These data imply equivalent roles for DevS and DosT in NO signaling, with positive regulation of the dormancy regulon by PhoP leading to a basal level of DevS expression under aerobic conditions (11, 15).

The ability of DevS and DosT to respond to NO under aerobic conditions is particularly interesting. The NO dioxygenation (NOD) reaction that converts NO to relatively harmless nitrate has been implicated as a major mechanism for relieving nitrosative stress in bacteria (16, 17). This reaction is catalyzed by the oxy-heme groups of flavohemoglobins and truncated hemoglobins in bacteria as well as myoglobin and hemoglobin in mammals (18). In *Mycobacterium bovis*, a truncated hemoglobin HbN possesses NOD activity and confers NO resistance (19). The HbN homologue of MTB performs the same function when expressed in heterologous hosts (20). Although DevS and DosT are unlikely to function catalytically as detoxification enzymes, the NOD reaction could provide a mechanism for termination of the kinase inhibition imposed by the ferrous–dioxy complex.

MATERIALS AND METHODS

Protein Expression and Purification. Full-length DevS and DosT were obtained as His-tagged constructs as described in ref 21. Activity and spectroscopy measurements of full-length DevS were unchanged by the presence of the His tag, but removal with TEV protease was required with full-length DosT as the presence of this tag was previously observed to affect the ligation and spin states of the Fe(II) heme.²

Protein and NO Solutions. Protein solutions were prepared in 50 mM phosphate buffer (pH 7.5) with 150 mM NaCl and purged with argon before being brought into a glovebox with a controlled atmosphere of <1 ppm O₂ (Omni-Lab System, Vacuum Atmospheres Co.). Reduction to the heme Fe(II) protein was achieved by addition of a 5-fold excess of sodium dithionite followed by passage through a Sephadex G-25 desalting column (GE Healthcare). Complete heme reduction and dithionite removal were confirmed by UV–vis spectroscopy with a Cary 50 spectrometer. Solutions were then transferred to sealed serum bottles and exposed to ¹⁶O₂ (Airgas). Formation of the oxy complex was confirmed by UV–vis spectroscopy, and the final protein concentration was determined. The serum bottles were then opened in the glovebox to release excess O₂ prior to the protein solution being loaded into rapid freeze quench (RFQ) syringes or gastight Hamilton syringes for transfer to the stopped-flow apparatus. For RFQ experiments, ¹⁴N¹⁶O (Airgas) and ¹⁵N¹⁶O (98% ¹⁵N and 95% ¹⁶O, Aldrich) solutions were prepared by serial additions of NO gas to a sealed vial of anaerobic buffer. Concentrations of NO in stock solutions were determined by titration with deoxymyoglobin. Solutions in sealed serum bottles

were drawn into RFQ syringes using a needle attachment within the glovebox. For stopped-flow experiments, a concentrated solution of diethylamine NONOate (Cayman Chemical) (8.7 mM) was diluted in anaerobic phosphate buffer and incubated for 1 h at room temperature within the Hamilton gastight syringe prior to being loaded into the stopped-flow apparatus.

Measurements of Nitrate and Nitrite Concentrations. Production of nitrate and nitrite from the reaction of oxy-DevS with NO was assessed using the Griess reagent and nitrite reductase (nitrate/nitrite colorimetric kit from Cayman Chemical). Specifically, saturated NO solutions were used to reach a final NO concentration of 30 μM in solutions of oxy-DevS and oxy-myoglobin ranging between 6 and 9 μM and in buffer blanks. Complete conversion of oxy-DevS to oxidized Fe(III) DevS was confirmed by UV–vis spectroscopy and matched the nitrate concentration deduced from the colorimetric measurement.

Autophosphorylation Assays. DevS and DosT protein solutions in 50 mM potassium phosphate buffer (pH 7.5) with 100 mM NaCl were purged with Ar and reduced with sodium dithionite. Excess dithionite was removed using desalting columns, and CO or O₂ gas was added to the appropriate samples. Fully oxidized Fe(III) protein solutions were obtained from incubation in 2 mM potassium ferricyanide followed by desalting using spin columns (Zebra, Pierce). NO gas was added to these samples directly prior to addition of ATP to generate the Fe(III)–NO complex. As an alternative route to the production of the Fe(III)–NO complex, NONOate was used to produce a 3-fold excess of NO. These operations were performed in the anaerobic glovebox. All samples, except the oxy and Fe(III) proteins, were loaded into septum-sealed microcentrifuge tubes. All 50 μL assay samples contained final concentrations of 5.0 μM protein, 100 mM Tris-HCl (pH 7.5), 50 mM KCl, and 5 mM MgCl₂, after the addition of ATP. The CO samples also included 500 μM sodium dithionite. Reactions were initiated by addition via syringe of a few microliters of a solution containing [γ -³²P]-ATP (4500 Ci/mmol) (MP Biomedicals) and Ar-purged, unlabeled ATP (Sigma) to a final concentration of 500 μM and 5–10 μCi. Our earlier work used a final ATP concentration of 200 μM and 10 μCi (10), but the higher ATP concentrations used in this study result in a significant increase in final autophosphorylation levels. Aliquots (10 μL) were removed at various time points and combined with 3.0 μL of stop buffer [208 mM Tris-HCl (pH 6.8), 8.3% SDS, 42% glycerol, 167 mM DTT, and 0.08% bromophenol blue]. These samples were run through a 12% polyacrylamide gel, which was vacuum-dried at 80 °C for 1.5 h, and exposed in a PhosphorImager cassette (Molecular Dynamics) for approximately 24–48 h. Levels of phosphorylated protein were imaged on a Typhoon Trio+ PhosphorImager (Amersham Biosciences) and quantified according to the method of Nakamura et al. (22), except that the correction factor of 1.65 was eliminated because gels were completely dried. After exposure, dried gels were rehydrated in a 20% methanol/5% acetic acid solution and Coomassie stained to confirm consistency in the amount of protein loaded and the integrity of full-length proteins.

Stopped-Flow UV–Vis Spectroscopy. Oxy-DevS, Oxy-DosT, and NO solutions were generated as described above and loaded into an SX20 stopped-flow UV–vis spectrometer (Applied Photophysics) equipped with a photodiode array detector and a water bath equilibrated to 4.2 °C to collect spectral data from 4 ms to 4 s. The purity of the oxy form of the enzymes was confirmed by UV–vis spectroscopy prior to the enzymes

²E. T. Yukl, A. Ioanoviciu, S. Sivaramakrishnan, R. R. Ortiz de Montellano, and P. Moënne-Loccoz, unpublished results, 2010.

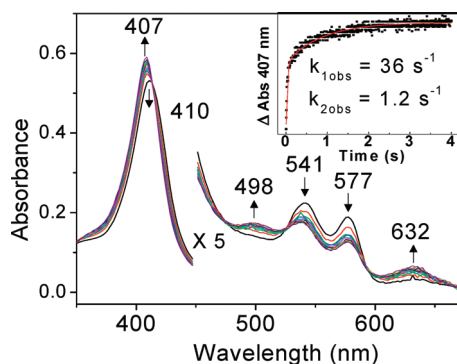


FIGURE 1: Stopped-flow UV-vis absorption spectra of the reaction of 4 μM oxy-DevS with 2 μM NO at 4.2 $^{\circ}\text{C}$ and pH 7.5. The inset shows the kinetics of the reaction measured at 407 nm.

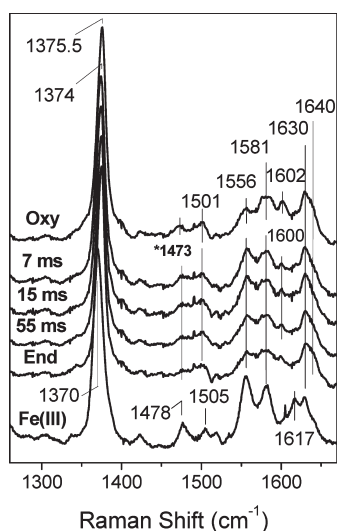


FIGURE 2: High-frequency RR spectra of RFQ samples of the reaction of 300 μM oxy-DevS with excess NO compared to those of resting oxy-DevS (top trace) and Fe(III)-DevS (bottom trace) ($\lambda_{\text{exc}} = 413$ nm, 20 mW, sample temperature of ~ 105 K). The 1473 cm^{-1} Raman band in the spectra of RFQ samples is assigned to residual frozen ethane.

being loaded into the stopped-flow instrument; excess solutions in the loading syringes were recovered from the stopped-flow apparatus after the experiments to confirm the stability of the oxy complexes in the absence of NO.

Rapid Freeze Quench (RFQ). Solutions were generated as described above and were loaded into the System 1000 Chemical/Freeze Quench Apparatus (Update Instruments, Inc.) equipped with a water bath maintained at 3–4 $^{\circ}\text{C}$. Reaction times were controlled by varying the syringe displacement rate from 2 to 8 cm/s or by varying the volume of the reactor hose after the mixer. Five milliseconds was added to the calculated reaction times to account for time of flight and freezing in liquid ethane. Samples (250 μL) were ejected into a glass funnel attached to EPR tubes filled with liquid ethane at a temperature of no higher than -120 $^{\circ}\text{C}$. The frozen sample was packed into the tube as the assembly sat within a Teflon block cooled with liquid nitrogen to a temperature no higher than -100 $^{\circ}\text{C}$. Liquid ethane was removed by immersion of the tubes in ethanol cooled to approximately -100 $^{\circ}\text{C}$ and application of vacuum for 5–10 min. Resonance Raman (RR) analysis before and after the removal of cryosolvent showed no perturbation in spectra because of this treatment.

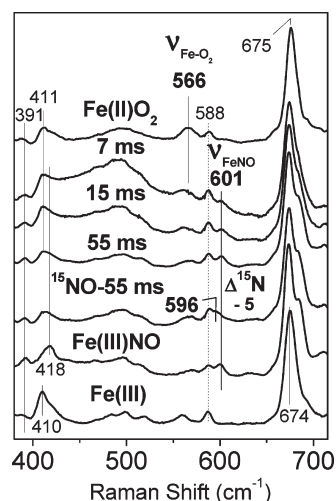


FIGURE 3: Low-frequency RR spectra of RFQ samples of the reaction of 300 μM oxy-DevS with excess NO compared to those of resting oxy-DevS (top trace) and Fe(III)NO-DevS and Fe(III)-DevS (bottom two traces). The spectrum of an RFQ sample frozen after 55 ms for the same reaction but with excess ^{15}N is also shown ($\lambda_{\text{exc}} = 413$ nm, 20 mW, sample temperature of ~ 105 K).

Successful mixing and NO dioxygenation reaction were confirmed by UV-vis analysis of samples ejected into a microcentrifuge tube, and by RR analysis of samples shot into a room-temperature NMR tube and frozen manually. These manually frozen samples and resting Fe(II)O₂, Fe(III), and Fe(III)NO were used to acquire low-temperature RR spectra of resting states for comparison with spectra of RFQ samples.

RR Spectroscopy. Low-temperature RR spectra were recorded using a backscattering geometry on RFQ samples and control samples in EPR tubes maintained at ~ 105 K in a liquid nitrogen coldfinger. All spectra were recorded on a custom McPherson 2061/207 spectrograph (0.67 m with variable gratings) equipped with a Princeton Instruments liquid N₂-cooled CCD detector (LN-1100PB) as described previously. Excitation at 413 nm was provided by a krypton laser (Innova 302, Coherent), and a Kaiser Optical supernotch filter was used to attenuate Rayleigh scattering. Frequencies were calibrated relative to indene and CCl₄ and are accurate to ± 1 cm^{-1} .

RESULTS AND DISCUSSION

Stopped-flow analyses of the reactions of oxy-DevS with substoichiometric amounts of NO show conversion of the oxy complexes to Fe(III) hemes (Figure 1). Specifically, while the initial oxy-DevS solution exhibits characteristic absorptions at 414, 541, and 577 nm (see Materials and Methods), the first stopped-flow trace obtained 4 ms after mixing of oxy-DevS with NO, and subsequent traces, show a decrease of these absorbance features in favor of a Soret maximum at 407 nm and absorption at 498 and 632 nm that are consistent with formation of Fe(III)-DevS. Despite our efforts to maximize the anaerobicity of the stopped-flow instrument, reproducing precise NO concentrations in the low micromolar range was not feasible in the absence of an anaerobic chamber confining the apparatus. Consequently, NO concentrations were inferred from the amount of oxy complex consumed after mixing. At 2 μM NO, the rate of the reaction with oxy-DevS at pH 7.5 was observed to be biphasic with k_{obs} values of 36 and 1.2 s^{-1} (Figure 1). Analysis of total nitrate and nitrite concentrations confirmed the quantitative conversion of NO to NO₃[−] by oxy-DevS (data not shown), as

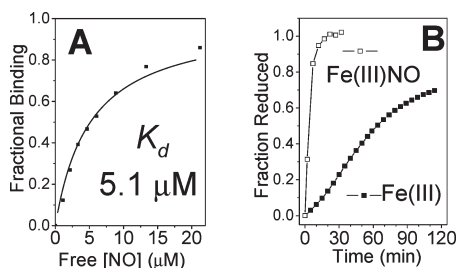


FIGURE 4: Binding curve determined from the titration of anoxic Fe(III)-DevS with NO (A) and reduction time course of 4.5 μM Fe(III)-DevS with 10 mM ascorbate in the presence and absence of 25 μM NO (B).

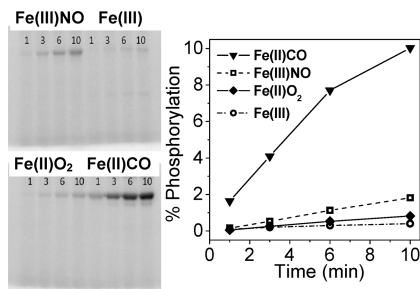


FIGURE 5: Autophosphorylation of 5 μM DevS in the presence of 500 μM ATP.

observed previously for oxymyoglobin and *M. bovis* HbN (19). Thus, despite technical limitations preventing adequate measurements in determining the second-order rate constants of this reaction, the existing results clearly demonstrate efficient NOD reactivity in the sensor kinase DevS.

The NOD reaction in DevS was also monitored by RFQ and RR spectroscopy, techniques that we have used together successfully to trap and characterize an Fe(III)–nitrate complex in the NOD reaction of myoglobin at pH 9.5 (23). The high-frequency RR spectra of 300 μM oxy-DevS mixed with excess NO and frozen at 7, 15, and 55 ms are nearly identical to that of the oxy complex (Figure 2). Specifically, the porphyrin ν_4 , ν_3 , ν_2 , and ν_{10} modes are observed at 1374, 1501, 1581, and 1640 cm^{-1} , respectively, and are characteristic of six-coordinate low-spin (6cLS) Fe(III) heme species (24). In contrast, the Fe(III) heme of DevS is predominantly 6cHS with ν_4 , ν_3 , and ν_{10} modes at 1370, 1478, and 1617 cm^{-1} , respectively.

The low-frequency RR spectra of the RFQ samples show a rapid consumption of the oxy complex, as determined by the loss of the $\nu(\text{Fe}-\text{O}_2)$ band at 566 cm^{-1} in the 7 ms RFQ sample (Figure 3). This mode was previously observed at 563 cm^{-1} in wt DevS at room temperature (10, 25). The loss of the $\nu(\text{Fe}-\text{O}_2)$ band is accompanied by the gradual appearance of a mode at 601 cm^{-1} , which downshifts by 5 cm^{-1} when the NO solution is substituted with ^{15}NO (Figure 3). The observed frequency and ^{15}N isotope shift are consistent with the assignment of this mode to a $\nu(\text{Fe}-\text{NO})$ band from an Fe(III)–NO complex (26–28). These assignments are consistent with the RR spectra of resting oxy-DevS, Fe(III)-DevS, and Fe(III)–NO DevS (Figure 3). Thus, the RR spectra of the RFQ samples provide evidence of the rapid decay of the oxy complex upon its reaction with excess NO to generate an Fe(III) state that can further react with excess NO to form a stable Fe(III)–NO complex.

The RFQ–RR data suggest that Fe(III)-DevS has an unusually high affinity for NO, and indeed, titration of an anoxic

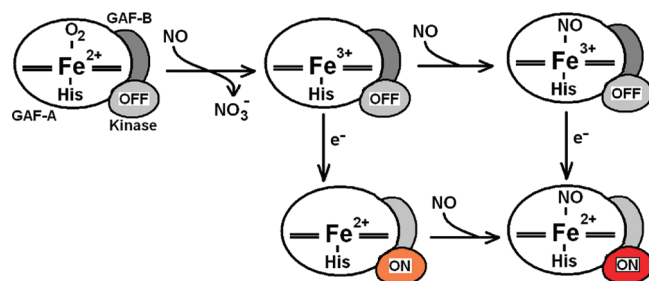


FIGURE 6: Proposed mechanism of kinase activation in the reaction of oxy-DevS with NO. The kinase domain is colored gray when inhibited, orange for the intermediate autokinase activity observed in deoxy-DevS, and red for the full activation observed with the Fe(II)–NO complex.

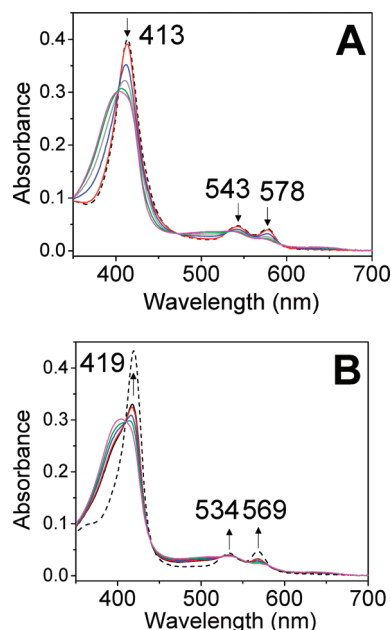


FIGURE 7: Room-temperature time course of the reaction of oxy-DosT with 1.33 equiv of DEA-NONOate at pH 7.4 (DEA-NONOate generates 1.5 equiv of NO with a $t_{1/2}$ of ~16 min). Panel A shows the first 21 min of the reaction, while panel B corresponds to the subsequent 30 min. Reference spectra of oxy-DosT (A) and Fe(III)NO-DosT (B) are also shown (black dashed lines).

solution of Fe(III)-DevS with a solution of NO yields an apparent K_d of ~5 μM (Figure 4A). This unusually high NO affinity exhibited by an Fe(III) heme protein (28) suggests that the Fe(III)–NO state could be physiologically relevant in the infected macrophage. The Fe(III)–NO complex of DevS shows only marginal activity in autophosphorylation assays compared to that of oxy-DevS (Figure 5) (8), but we have found that the Fe(III)–NO complex is easily reduced with 10 mM ascorbate, i.e., ~20-fold faster than the Fe(III)-DevS state (Figure 4B). Thus, reduction of the Fe(III)–NO complex to the Fe(II)–NO complex can be expected to be a rapid process in the reducing cellular environment and would lead to the activation of the kinase domain. As such, the NOD reaction of oxy-DevS may represent a rapid switching mechanism for converting an inactive oxy state to an active Fe(II)–NO species via formation of the Fe(III) and Fe(III)–NO complexes (Figure 6).

Given the possible early sensing role of DosT, the reactivity of its oxy form with NO and the NO affinity of its Fe(III) state are also of interest. Preliminary stopped-flow monitoring of the reaction of oxy-DosT with NO (at 0.57 μM) revealed a monophasic

reaction with a k_{obs} of $\sim 1 \text{ s}^{-1}$ similar to the slower component of the biphasic rate observed in DevS (data not shown), but no further stopped-flow experiments were conducted with DosT because activity measurements revealed the poor stability of the DosT protein. Instability of ferricyanide-oxidized DosT and its tendency to precipitate also prevent an accurate assessment of its affinity for NO. Despite problems of stability with DosT, the efficiency of the reaction of oxy-DosT with NO under aerobic conditions could be documented using the slow NO donor DEA-NONOate (Figure 7). Specifically, as a first equivalent of NO is produced, the conversion of oxy-DosT to the Fe(III) state is confirmed by the decrease in Soret absorption at 413 nm and the loss of well-resolved α - and β -bands at 578 and 543 nm in favor of the less distinctive absorption features of the oxidized protein (Figure 7A). Subsequent production of NO beyond 1 equiv results in an increased Soret absorption at 419 nm (Figure 7B), an observation consistent with partial conversion of the Fe(III) state to the Fe(III)–NO complex despite the competing reaction of molecular oxygen with NO. The amount of the Fe(III)–NO complex formed in these experiments suggests an upper limit of 1 μM for the K_d in Fe(III)–DosT.

CONCLUSION

Previous studies have shown that the complexes of CO and NO with ferrous DevS and DosT activate the autophosphorylation that eventually leads to induction of the dormancy regulon. In contrast, the dioxygen complex has negligible autophosphorylation activity (8–10). Ferric DevS, like the dioxygen complex, does not significantly autophosphorylate, but the ligand-free ferrous form exhibits intermediate autophosphorylation activity. Thus, one mechanism for induction of the dormancy regulon includes a transition to a sufficiently low O_2 tension such that the ferrous protein is unliganded or competitively coordinated by CO. The situation with NO differs, because NO has potent antimycobacterial properties, and exposure to this gas can occur abruptly, requiring a rapid response. These results suggest that NO initiates a dormancy response not by exchanging with oxygen as the ligand to the heme Fe(II) but rather by reacting with the Fe(II)– O_2 complex to produce a heme Fe(III) or heme Fe(III)–NO complex, if the concentration of NO is in the micromolar range. Both Fe(III) and Fe(III)–NO states can be subsequently reduced to the Fe(II) and Fe(II)–NO states, respectively. We have previously identified a redox partner in *M. tuberculosis* that can reduce ferric DevS to the ferrous state and can therefore presumably also reduce the ferric NO complex. In this regard, it is useful to note that the Fe(III)–NO form is much more easily reduced by ascorbate than the unliganded Fe(III) form. Because the Fe(II)–NO complex is highly activated for autophosphorylation (8–10), the net result of the exposure of DevS– O_2 to NO is a rapid initiation of the dormancy response.

REFERENCES

- Choi, H. S., Rai, P. R., Chu, H. W., Cool, C., and Chan, E. D. (2002) Analysis of nitric oxide synthase and nitrotyrosine expression in human pulmonary tuberculosis. *Am. J. Respir. Crit. Care Med.* 166, 178–186.
- Wayne, L. G., and Sohaskey, C. D. (2001) Nonreplicating persistence of *Mycobacterium tuberculosis*. *Annu. Rev. Microbiol.* 55, 139–163.
- Cunningham, A. F., and Spreadbury, C. L. (1998) Mycobacterial stationary phase induced by low oxygen tension: Cell wall thickening and localization of the 16-kilodalton α -crystallin homolog. *J. Bacteriol.* 180, 801–808.
- Sherman, D. R., Voskuil, M., Schnappinger, D., Liao, R., Harrell, M. I., and Schoolnik, G. K. (2001) Regulation of the *Mycobacterium tuberculosis* hypoxic response gene encoding α -crystallin. *Proc. Natl. Acad. Sci. U.S.A.* 98, 7534–7539.
- Voskuil, M. I., Schnappinger, D., Visconti, K. C., Harrell, M. I., Dolganov, G. M., Sherman, D. R., and Schoolnik, G. K. (2003) Inhibition of respiration by nitric oxide induces a *Mycobacterium tuberculosis* dormancy program. *J. Exp. Med.* 198, 705–713.
- Dasgupta, N., Kapur, V., Singh, K. K., Das, T. K., Sachdeva, S., Jyothisri, K., and Tyagi, J. S. (2000) Characterization of a two-component system, devR-devS, of *Mycobacterium tuberculosis*. *Tubercle and Lung Disease* 80, 141–159.
- Roberts, D. M., Liao, R. P., Wisedchaisri, G., Hol, W. G., and Sherman, D. R. (2004) Two sensor kinases contribute to the hypoxic response of *Mycobacterium tuberculosis*. *J. Biol. Chem.* 279, 23082–23087.
- Kumar, A., Toledo, J. C., Patel, R. P., Lancaster, J. R., Jr., and Steyn, A. J. C. (2007) *Mycobacterium tuberculosis* DosS is a redox sensor and DosT is a hypoxia sensor. *Proc. Natl. Acad. Sci. U.S.A.* 104, 11568–11573.
- Sousa, E. H., Tuckerman, J. R., Gonzalez, G., and Gilles-Gonzalez, M. A. (2007) DosT and DevS are oxygen-switched kinases in *Mycobacterium tuberculosis*. *Protein Sci.* 16, 1708–1719.
- Yukl, E. T., Ioanoviciu, A., Nakano, M. M., de Montellano, P. R., and Moënne-Loccoz, P. (2008) A distal tyrosine residue is required for ligand discrimination in DevS from *Mycobacterium tuberculosis*. *Biochemistry* 47, 12532–12539.
- Honaker, R. W., Leistikow, R. L., Bartek, I. L., and Voskuil, M. I. (2009) Unique roles of DosT and DosS in DosR regulon induction and *Mycobacterium tuberculosis* dormancy. *Infect. Immun.* 77, 3258–3263.
- Cho, H. Y., Cho, H. J., Kim, Y. M., Oh, J. I., and Kang, B. S. (2009) Structural insight into the heme-based redox sensing by DosS from *Mycobacterium tuberculosis*. *J. Biol. Chem.* 284, 13057–13067.
- Ioanoviciu, A., Mehareenna, Y. T., Poulos, T. L., and Ortiz de Montellano, P. R. (2009) DevS oxy complex stability identifies this heme protein as a gas sensor in *Mycobacterium tuberculosis* dormancy. *Biochemistry* 48, 5839–5848.
- Saini, D. K., Malhotra, V., and Tyagi, J. S. (2004) Cross talk between DevS sensor kinase homologue, Rv2072c, and DevR response regulator of *Mycobacterium tuberculosis*. *FEBS Lett.* 565, 75–80.
- Gonzalo-Asensio, J., Mostowy, S., Harders-Westervreen, J., Huygen, K., Hernandez-Pando, R., Thole, J., Behr, M., Gicquel, B., and Martin, C. (2008) PhoP: A missing piece in the intricate puzzle of *Mycobacterium tuberculosis* virulence. *PLoS One* 3, e3496.
- Poole, R. K., and Hughes, M. N. (2000) New functions for the ancient globin family: Bacterial responses to nitric oxide and nitrosative stress. *Mol. Microbiol.* 36, 775–783.
- Brunori, M. (2001) Nitric oxide moves myoglobin centre stage. *Trends Biochem. Sci.* 26, 209–210.
- Gardner, P. R. (2005) Nitric oxide dioxygenase function and mechanism of flavohemoglobin, hemoglobin, myoglobin and their associated reductases. *J. Inorg. Biochem.* 99, 247–266.
- Ouellet, H., Ouellet, Y., Richard, C., Labarre, M., Wittenberg, B., Wittenberg, J., and Guertin, M. (2002) Truncated hemoglobin HbN protects *Mycobacterium bovis* from nitric oxide. *Proc. Natl. Acad. Sci. U.S.A.* 99, 5902–5907.
- Pathania, R., Navani, N. K., Gardner, A. M., Gardner, P. R., and Dikshit, K. L. (2002) Nitric oxide scavenging and detoxification by the *Mycobacterium tuberculosis* haemoglobin, HbN in *Escherichia coli*. *Mol. Microbiol.* 45, 1303–1314.
- Ioanoviciu, A., Yukl, E. T., Moënne-Loccoz, P., and Ortiz de Montellano, P. R. (2007) DevS, a heme-containing two-component oxygen sensor of *Mycobacterium tuberculosis*. *Biochemistry* 46, 4250–4260.
- Nakamura, H., Saito, K., and Shiro, Y. (2001) Quantitative measurement of radioactive phosphorylated proteins in wet polyacrylamide gels. *Anal. Biochem.* 294, 187–188.
- Yukl, E. T., de Vries, S., and Moënne-Loccoz, P. (2009) The millisecond intermediate in the reaction of nitric oxide with oxymyoglobin is an iron(III)-nitrate complex, not a peroxynitrite. *J. Am. Chem. Soc.* 131, 7234–7235.
- Spiro, T. G., and Li, X. Y. (1988) Resonance Raman spectroscopy of metalloporphyrins. In *Biological Applications of Raman Spectroscopy*. Volume 3. Resonance Raman Spectra of Hemes and Metalloproteins (Spiro, T. G., Ed.) pp 1–37, John Wiley & Sons, New York.
- Yukl, E. T., Ioanoviciu, A., de Montellano, P. R., and Moënne-Loccoz, P. (2007) Interdomain interactions within the two-component

- heme-based sensor DevS from *Mycobacterium tuberculosis*. *Biochemistry* 46, 9728–9736.
26. Benko, B., and Yu, N. T. (1983) Resonance Raman studies of nitric oxide binding to ferric and ferrous hemoproteins: Detection of Fe(III)-NO stretching, Fe(III)-N-O bending, and Fe(II)-N-O bending vibrations. *Proc. Natl. Acad. Sci. U.S.A.* 80, 7042–7046.
27. Mukai, M., Ouellet, Y., Ouellet, H., Guertin, M., and Yeh, S. R. (2004) NO binding induced conformational changes in a truncated hemoglobin from *Mycobacterium tuberculosis*. *Biochemistry* 43, 2764–2770.
28. Wang, J., Lu, S., Moënne-Loccoz, P., and Ortiz de Montellano, P. R. (2003) Interaction of nitric oxide with human heme oxygenase-1. *J. Biol. Chem.* 278, 2341–2347.